SPACE SCIENCES


10.1126/sciadv.1501400

# Origin of uranium isotope variations in early solar nebula condensates

**François L. H. Tissot,* Nicolas Dauphas, Lawrence Grossman**

**High-temperature condensates found in meteorites display uranium isotopic variations ($^{235}U/^{238}U$), which complicate dating the solar system's formation, the origin of which remains mysterious. It is possible that these variations are due to the decay of the short-lived radionuclide $^{247}Cm$ ($t_{1/2}$ = 15.6 My) into $^{235}U$, but they could also be due to uranium kinetic isotopic fractionation during condensation. We report uranium isotope measurements of meteoritic refractory inclusions that reveal excesses of $^{235}U$ reaching ~6% relative to average solar system composition, which can only be due to the decay of $^{247}Cm$. This allows us to constrain the $^{247}Cm/^{235}U$ ratio at solar system formation to $(1.1 \pm 0.3) \times 10^{-4}$. This value provides new clues on the universality of the rapid neutron capture *r*-process of nucleosynthesis.**

## INTRODUCTION

All elements beyond the iron peak (above ~70 atomic mass units) are the products of three main processes of stellar nucleosynthesis: the *s*- (*slow* neutron capture), *r*- (*rapid* neutron capture), and *p*-process (*proton* process) (*1*, *2*). Unlike the *s*- and *p*-process, which are relatively well understood [neutron capture in asymptotic giant branch (AGB) stars for the *s*-process and photodisintegration of seed nuclei in supernovae for the *p*-process] (*3*, *4*), little is known regarding the astrophysical conditions under which *r*-process nuclides are produced (*5*–*8*). The *r*-process label may comprise some diversity as it was suggested that up to three *r*-processes were responsible for producing light *r*-nuclides (A < 140), heavy *r*-nuclides (A > 140), and actinides (for example, U and Th). The existence of an "actinide" production site is motivated by two main observations: (i) the ages of some old stars inferred from their Th/Eu ratios are negative, meaning that they must have formed with a Th/Eu ratio that was higher than that relevant to the solar system (SS) (*9*), and (ii) the abundance of the short-lived radionuclide (SLR) $^{244}Pu$ [$t_{1/2}$ = 79.3 million years (My)] in meteorites is low compared to another nominal *r*-process radionuclide, $^{182}Hf$ (*7*). However, $^{244}Pu$ has a long half-life and its stellar yield is uncertain (*10*), which makes it insensitive to the history of nucleosynthesis before SS formation and whether or not multiple *r*-process sites contributed to the synthesis of the actinides. In contrast, $^{247}Cm$, which decays into $^{235}U$, has a much shorter half-life ($t_{1/2}$ = 15.6 My) and would be very well suited to address this question. Unfortunately, its abundance in the early solar system (ESS) has been the subject of some debate that boils down to knowing whether the uranium isotope variations (that is, $^{235}U/^{238}U$ ratio) measured in early-formed nebular condensates [calcium- and aluminum-rich inclusions (CAIs)] are due to the decay of $^{247}Cm$ or isotopic fractionation during condensation. The two cannot be easily distinguished because U has only two long-lived isotopes and both mechanisms would produce similar correlations between light U isotope enrichments and U concentrations.

Recently, excesses in $^{235}U$ of up to 3.5‰ were documented in four fine-grained CAIs (*11*). To demonstrate that those variations are due to $^{247}Cm$ decay, one must show that the $\delta^{235}U$ values correlate with the Cm/U parent-to-daughter ratios. Because Cm has no long-lived isotopes, another element must be used as a proxy for Cm in isochron diagrams. On the basis of their near-identical valence states, ionic radii, and volatilities, the light rare earth elements (REEs) are thought to behave similarly to Pu and Cm during nebular processes (*12*–*14*). This conclusion is supported by the observed coherent behavior of Pu, Nd, and Sm in pyroxene/melt and phosphate/melt partitioning experiments (*15*) and during magmatic differentiation in achondrites (*12*, *14*). Although Th has sometimes been used as a proxy for Cm (*11*, *16*), coherent behavior for the Th-Cm and Th-Pu pairs is neither expected (*13*) nor observed (*12*), and the light REEs (for example, Nd or Sm) are therefore taken as more reliable Cm proxies. The $^{235}U$ excesses observed by Brennecka *et al.* (*11*) correlate with Nd/U ratios, which the authors interpreted as evidence of live $^{247}Cm$ in the ESS at a level of $(^{247}Cm/^{235}U)_{ESS}$ = (1.1 to 2.4) × $10^{-4}$. However, such $^{235}U$ enrichments could also reflect mass-dependent fractionation during condensation of solid CAIs from nebular gas (*17*–*19*). Indeed, the kinetic theory of gases predicts that the lighter isotope ($^{235}U$) should condense faster than the heavier isotope ($^{238}U$), resulting in fractionations that can reach $\sqrt{238/235} \sim 6‰$ for condensation of atomic U in a low-pressure gas. If only a fraction of the U initially present in the gas condensed, as inferred for fine-grained CAIs that are depleted in U, then kinetic isotopic fractionation may be expressed. One would expect to find a correlation between U isotopic variations and the degree of U depletion in both cases of $^{247}Cm$ decay and fractionation during condensation, so it is presently undecided which mechanism is responsible for the U isotope variations documented in CAIs.

Definitive evidence of live $^{247}Cm$ therefore awaits the discovery of meteoritic material that is highly depleted in uranium and displays $^{235}U$ excess outside of the ±6‰ window allowed by fractionation at condensation. Because the abundance of $^{247}Cm$ in the ESS is expected to be low (*10*), such large excesses of $^{235}U$ from $^{247}Cm$ decay will only be resolvable in phases with $^{144}Nd/^{238}U$ ratios exceeding ~1300. Therefore, numerous slabs of the Allende meteorite were examined, and 15 CAIs (12 fine-grained and 3 coarse-grained) were extracted and digested with acids. Many of these CAIs revealed group II REE patterns and large U depletions indicative of incomplete condensation of refractory lithophile elements (see the Supplementary Materials). A method was developed to measure accurately the U isotopic compositions of samples with low U contents (0.1 to 0.01 ng; see the Supplementary Materials).

Origins Lab, Department of the Geophysical Sciences, and Enrico Fermi Institute, University of Chicago, Chicago, IL 60637, USA.
*Corresponding author. E-mail: ftissot@uchicago.edu

## RESULTS

As in previous studies, most samples display low $^{144}Nd/^{238}U$ ratios (that is, <600), and their $\delta^{235}U$ values are within 6‰ of the bulk SS value at $\delta^{235}U$ = +0.31‰ (relative to CRM-112a) (*19*, *20*). These samples display a trend between $\delta^{235}U$ and $^{144}Nd/^{238}U$ similar to that described previously on similar samples (*11*) and which had been taken as evidence that $^{247}Cm$ was alive in the ESS. The samples display significant scatter around the best-fit line that cannot be entirely explained by analytical uncertainty [the mean square weighted deviation (MSWD) of the regression for samples with $^{144}Nd/^{238}U$ ratios lower than 600 is 46]. Even coarse-grained CAIs that are nondepleted in U (low $^{144}Nd/^{238}U$ ratios) have $\delta^{235}U$ that vary between −0.16 and +1.35‰, well outside of analytical uncertainty.

One sample (named Curious Marie) has an extremely high $^{144}Nd/^{238}U$ ratio (~13,720) and a $^{235}U$ excess of +58.9 ± 1.9‰ (equivalent to an absolute $^{238}U/^{235}U$ ratio of 130.17 ± 0.27; Fig. 1 and Table 1). For comparison, the highest $^{144}Nd/^{238}U$ ratio and $^{235}U$ excess measured in CAIs prior to this work were 481 and +3.43‰ ($^{238}U/^{235}U$ = 137.37), respectively (*11*). Considerable effort was expended to confirm this result (see the Supplementary Materials). The measurement was triplicated using different sample purification schemes and various measurement setups. The tests yielded $\delta^{235}U$ values of +52.79 ± 14.91‰ after one purification step with $^{235}U$ measured on Faraday, +59.12 ± 2.80‰ after two purifications with $^{235}U$ on an electron multiplier, and +58.97 ± 2.72‰ after three purifications with $^{235}U$ on an electron multiplier. Extensive testing was also done to ensure that no interferences or matrix effects were affecting the measurement by combining the matrix cut from Curious Marie with CRM-112a, purifying the U by column chemistry, and finding that the measured U isotopic composition is correct (that is, identical to pure CRM-112a) after purification.

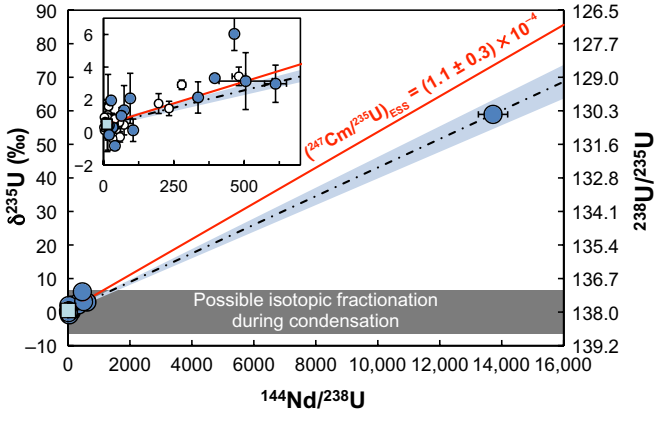


**Fig. 1. $\delta^{235}U$ plotted as a function of the $^{144}Nd/^{238}U$ ratio in meteoritic samples.** Open circles, previous studies (*11*, *17*–*19*, *33*, *34*); blue circles, Allende CAIs from this work; light-blue square, bulk Allende from this work]. The +59‰ $\delta^{235}U$ value observed in the Curious Marie CAI is well outside the range of variations expected from fractionation during condensation (gray rectangle) and is thus interpreted as definitive evidence for live $^{247}Cm$ in the ESS. The scatter in the data (for example, at very low Nd/U ratios) suggests that stable isotopic fractionation during evaporation/condensation also influenced the U isotopic composition of CAIs. The slope of the two-point isochron between Curious Marie and the rest of the samples translates into a $^{247}Cm/^{235}U$ of $(0.9 \pm 0.07) \times 10^{-4}$ at the time of Nd/U fractionation in Curious Marie. Accounting for a possible delay between this fractionation event (possibly related to the extensive alteration of this CAI) and the formation of the SS of 5 ± 5 My, the inferred $^{247}Cm/^{235}U$ at SS formation is $(1.1 \pm 0.3) \times 10^{-4}$ (red line).

## DISCUSSION

### Evidence for $^{247}Cm$

The finding of such a large excess $^{235}U$ in a normal CAI [in opposition to fractionated and unknown nuclear (FUN) CAIs, which is a group of refractory inclusions that display FUN effects; see the Supplementary Materials] can only be explained by decay of $^{247}Cm$ into $^{235}U$. Below, we examine other processes that could potentially lead to U isotope variations in ESS materials and show that they all suffer from serious shortcomings:

(i) Isotopic fractionation during secondary processes (for example, aqueous alteration and/or redox processes), either on the meteorite parent body or on Earth, can impart large isotopic fractionation to light elements (such as Li). However, the degree of fractionation generally decreases as the mass of the element increases, and for U on Earth, the variations are limited to ~1.5 to 2‰ (*21*). Although this process could lead to some scatter in the data around the isochron, it cannot explain a 59‰ anomaly.

(ii) Large isotopic variations of nucleosynthetic origin have been documented for refractory elements in CAIs and are usually readily identified as departures from mass-dependent fractionation. For uranium, which has only two stable isotopes, it is impossible to distinguish between $^{247}Cm$ decay and nucleosynthetic anomalies. Nevertheless, considering that anomalies on the order of a few permil in heavy elements (for example, Ba, Sm, and Nd) are only found in FUN CAIs (normal CAIs have more subdued anomalies of a few tenths of permil) and given that Curious Marie ($\delta^{238}U$ ~ 59‰) is not a FUN CAI (see the Supplementary Materials), the large $^{235}U$ excess found here cannot be reasonably ascribed to the presence of nucleosynthetic anomalies.

(iii) Finally, U isotopic fractionation could be the result of fractionation during evaporation/condensation processes. During condensation, the light isotope of U condenses faster, leading to large $^{235}U$ depletion in the condensing gas and the instantaneous solid, but $^{235}U$ excesses limited to +6‰ (see the Supplementary Materials). Similarly, during evaporation, the highest $^{235}U$ excess predicted by the kinetic theory of gases is limited to ~6‰. Consequently, evaporation/condensation processes cannot explain the 59‰ $^{235}U$ excess observed in Curious Marie, which leaves $^{247}Cm$ decay as the only possible explanation.

### Closure time in Curious Marie and $^{247}Cm/^{235}U$ ratio in the ESS

The large excess of $^{235}U$ found in the Curious Marie CAI is definitive evidence that $^{247}Cm$ was alive in the ESS. An initial ($^{247}Cm/^{235}U$) ratio of $\sim 0.9 \times 10^{-4}$ at the time of closure can be calculated using the slope of the isochron in Fig. 1. Even though the samples with low $^{144}Nd/^{238}U$ ratios define a trend with $\delta^{235}U$, the slope of the isochron in Fig. 1 is mainly leveraged by Curious Marie ($^{144}Nd/^{238}U$ ratio ~ 13,720). The initial $^{247}Cm/^{235}U$ ratio of $(0.9 \pm 0.07) \times 10^{-4}$ thus corresponds to the time when this CAI acquired its high $^{144}Nd/^{238}U$ ratio. Terrestrial alteration is ruled out because the Allende meteorite is an observed fall that did not experience much terrestrial weathering. The extreme uranium depletion in the Curious Marie CAI is thus most likely due to solar nebula condensation and/or nebular/parent body alteration. All fine-grained CAIs in this study display a typical group II

**Table 1. Type, REE pattern, mass, U content, $^{144}Nd/^{238}U$ ratio, and U isotopic composition of the samples analyzed in this study.** *n* is the number of replicate analyses for each sample (starting from solutions). Nd/U ratios and isotopic compositions are corrected for blank contributions (see table S2). $\delta^{235}U = [(^{235}U/^{238}U)_{sample}/(^{235}U/^{238}U)_{CRM\text{-}112a} - 1] \times 10^3$. Error bars are 95% confidence intervals. Nd/U ratio was calculated using the U concentration from the double-spike technique, and Nd concentration from the standard addition technique (see the Supplementary Materials).

| Average $^{144}Nd/^{238}U$ ratios and U isotopic compositions of CAIs | | | | | | | | | |
|---|---|---|---|---|---|---|---|---|---|
| **Sample** | **Type** | **REE pattern** | **Mass (mg)** | **U (ng)** | ***n*** | **$^{144}Nd/^{238}U$** | **±** | **$\delta^{235}U$ (‰) blk corr.** | **±** |
| Allende | CV3 | | 1016 | 21.9 | 2 | 12.2 | 1.5 | 0.49 | 0.16 |
| FG-1 | Fine-gr. CAI | Group II | 35.2 | 0.77 | 2 | 95.0 | 7.0 | 2.08 | 1.54 |
| Curious Marie | Fine-gr. CAI | Group II | 717.9 | 0.37 | 3 | 13720 | 472 | 58.94 | 1.93 |
| CG-1 | Coarse-gr. CAI | Group I | 48.4 | 0.76 | 2 | 73.2 | 5.3 | 1.35 | 1.52 |
| FG-2 | Fine-gr. CAI | Group II | 50.4 | 1.53 | 2 | 105.4 | 3.9 | 0.12 | 0.69 |
| FG-3 | Fine-gr. CAI | Group II | 98.3 | 4.05 | 2 | 63.5 | 2.7 | 1.01 | 0.50 |
| FG-4 | Fine-gr. CAI | Group II | 349.7 | 15.7 | 2 | 40.5 | 2.9 | −0.83 | 0.25 |
| FG-5 | Fine-gr. CAI | Group II | 48.7 | 2.82 | 2 | 32.9 | 2.4 | 0.30 | 0.59 |
| FG-6 | Fine-gr. CAI | Group II | 54.9 | 0.35 | 2 | 612 | 39 | 2.98 | 1.14 |
| FG-7 | Fine-gr. CAI | Group II | 61.4 | 0.98 | 2 | 336 | 10 | 2.13 | 0.96 |
| FG-8 | Fine-gr. CAI | Group II | 377.3 | 8.50 | 2 | 395 | 6 | 3.32 | 0.21 |
| FG-9 | Fine-gr. CAI | Group II | 330.7 | 23.9 | 2 | 26.8 | 1.9 | 1.95 | 0.14 |
| FG-10 | Fine-gr. CAI | Group II | 15.61 | 0.24 | 2 | 505 | 95 | 3.14 | 1.75 |
| CG-2 | Coarse-gr. CAI | Group V | 200.4 | 23.0 | 2 | 19.1 | 1.4 | 0.43 | 0.14 |
| FG-11 | Fine-gr. CAI | Group II | 68.6 | 0.83 | 2 | 165 | 10. | 6.03 | 1.02 |
| TS32 | Coarse-gr. CAI | Group V | 41.8 | 4.89 | 2 | 197 | 1.4 | −0.16 | 0.30 |

REE pattern, thought to represent a snapshot in time and space of the condensation sequence (*22*, *23*). The most refractory REEs (heavy REEs except Tm and Yb) are depleted in these CAIs because they were sequestered in ultrarefractory dust such as perovskite or hibonite, whereas the more volatile REEs (Eu and Yb) and uranium are also depleted because they stayed in the gas phase when those CAIs formed. In most samples, U and Yb present similar levels of depletion relative to solar composition and the abundance of other refractory lithophile elements (Fig. 2), indicating that those two elements have similar behaviors during evaporation/condensation processes under solar nebula conditions. However, in Curious Marie, the U/Nd ratio is 1000 times lower than solar composition, whereas the Yb/Nd ratio is only depleted by a factor of 50. If U and Yb have similar behaviors during condensation, one would expect the U/Nd ratio to be 50 times lower than solar, not 1000 times as is observed. Compared to other fine-grained CAIs analyzed, Curious Marie is peculiar because it is extremely altered, which is manifested by the extensive replacement of high-T phases by low-T alteration products such as nepheline and sodalite [its $Na_2O$ is 15 weight percent (wt %) when other CAIs are all lower than 6.7 wt %; table S1]. Such alteration may have mobilized U, producing a 20-fold U depletion on top of the 50-fold depletion associated with condensation.

Some of these alteration products could have formed (i) in the nebula, (ii) on an earlier generation of water-rich asteroid, or (iii) during aqueous alteration on Allende itself [for example, Ross *et al.* (*24*) and Russell and MacPherson (*25*) and references therein]. Regardless of the location, dating of aqueous alteration products on meteorite parent bodies with extinct radionuclides $^{36}Cl$ ($t_{1/2}$ = 0.301 My), $^{26}Al$ ($t_{1/2}$ = 0.717 My), $^{53}Mn$ ($t_{1/2}$ = 3.74 My), or $^{129}I$ ($t_{1/2}$ = 15.7 My) suggests that it took place no later than 10 My after SS formation. This is a conservative upper limit because secondary alteration phases in fine-grained inclusions may have formed very early in the nebula. The half-life of $^{247}Cm$ is 15.6 My, meaning that a time span of ~5 ± 5 My between SS formation and CAI alteration (and possible U depletion) translates into a correction for the initial $^{247}Cm/^{235}U$ ratio of 25 ± 25% (the uncertainty on this factor takes into account the uncertainty on the closure age). Our present best estimate of the initial SS $^{247}Cm/^{235}U$ ratio is thus $(1.1 \pm 0.3) \times 10^{-4}$, which is equivalent to $(^{247}Cm/^{238}U)_{ESS} = (3.7 \pm 0.9) \times 10^{-5}$ and $(^{247}Cm/^{232}Th)_{ESS} = (1.6 \pm 0.4) \times 10^{-5}$. This value is in agreement with the $^{247}Cm/^{235}U$ ratio of (1.1 to 2.4) × $10^{-4}$ obtained by Brennecka *et al.* (*11*) based on CAI measurements and an upper limit of ~$4 \times 10^{-3}$ inferred from earlier meteoritic measurements (*26*). It is also in line with the lower limit derived from modeling of galactic chemical evolution (GCE) (*10*), which predicts an initial ratio of (5.0 ± 2.5) × $10^{-5}$.

## Fractionation of U isotopes during evaporation/condensation

Some of the samples with low $^{144}Nd/^{238}U$ ratios show significant scatter around the isochron (see inset of Fig. 1), outside of analytical uncertainties. In particular, samples with $^{144}Nd/^{238}U$ ratio as low as ~20 span a range of $\delta^{235}U$ values of 3.5‰, a feature that led previous

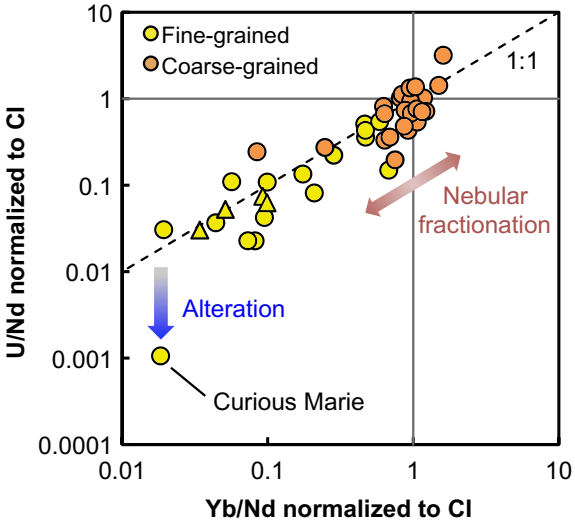


**Fig. 2. Correlation between U and Yb abundances relative to solar composition and the abundance of Nd (a refractory lithophile element).** Circles denote data from different studies (*35*–*37*) and this study, and triangles denote data from Brennecka *et al.* (*11*). This correlation indicates that U and Yb have similar behaviors during evaporation/condensation processes under solar nebula conditions. The Curious Marie CAI plots off the 1:1 line, with a CI-normalized U/Nd ratio 20 times lower than that of Yb/Nd. This CAI is extremely altered (see main text and table S1), and such alteration may have mobilized U, producing a 20-fold U depletion on top of the 50-fold depletion associated with condensation.

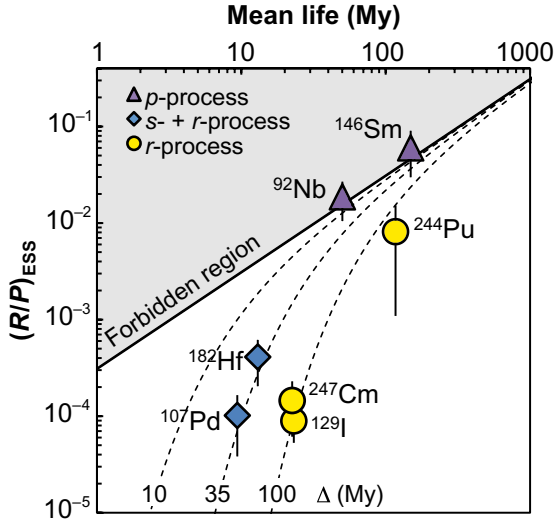


**Fig. 3. Meteoritic abundance ratios of extinct radionuclides to stable nuclides produced by the same process (for example, $^{129}I/^{127}I^{r}$), normalized to stellar production ratios versus mean lives ($\tau = t_{1/2}/\ln 2$).** The superscript "r" refers to the *r*-process component of the cosmic abundance [obtained after subtracting the *s*-process contribution from solar abundances (*3*)]. When the normalizing isotope is not stable (for example, $X/^{238}U$ or $X/^{232}Th$), the *R*/*P* ratio [that is, $(N_{SLR}/N_{Stable})/(P_{SLR}/P_{Stable})$] is corrected for the decay of the long-lived isotope by multiplication by the *N*/*P* ratio of the normalizing isotope in the ESS [0.71 for $^{238}U$ and 0.89 for $^{232}Th$, values from Nittler and Dauphas (*10*)]. Triangles denote *p*-process isotopes, diamonds denote *r*-process nuclides with possible large *s*-process contributions, and circles denote *r*-process isotopes. The data are compared to model steady-state abundances in the ISM, using the model of Dauphas *et al.* (*28*) with $k = 1.7$ and a presolar age of the galaxy of 8.7 Gy. Dotted curves show model abundances assuming free-decay intervals of 10, 35, and 100 My, respectively. The abundances of all *r*-process nuclides can be explained by a single *r*-process environment that was active throughout the history of the galaxy and from which the solar system parent material was isolated about 100 My before SS formation, provided that $^{182}Hf$ and $^{107}Pd$ in meteorites originate from the *s*-process (*6*, *31*). See the Supplementary Materials for source data.

workers (*17*, *18*) to question the conclusion of Brennecka *et al.* (*11*) that $^{247}Cm$ was responsible for U isotope variations. This scatter is most likely due to isotopic fractionation during condensation, suggesting that better isochronous behavior could be obtained if such fractionation could be corrected.

### Implications for the *r*-process

In addition to the dating implications that large $^{235}U/^{238}U$ variations have on the Pb-Pb ages of the CAIs (*11*, *21*), the existence of $^{247}Cm$ in the ESS has implications for the nucleosynthesis of *r*-process elements. The simplest GCE model that successfully reproduces the metallicity distribution of G-dwarfs requires infall of gas onto the galactic disk (*10*, *27*, *28*). In such a model, the abundance ratio of an SLR normalized to a stable nuclide is

$$\frac{N_{SLR}}{N_{Stable}} = \frac{P_{SLR}}{P_{Stable}} \cdot (k+1)\tau/T \qquad (1)$$

where $N$ is the abundance, $P$ is the production ratio, $\tau$ is the mean life of the SLR ($\tau = 1/\lambda$), $T$ is the age of the galaxy at the time when the ratio $N_{SLR}/N_{Stable}$ is to be calculated, and $k$ is a constant that distinguishes closed-box ($k = 0$) versus infall models (typically, $k = 2 \pm 1$) (*8*, *27*–*29*). If $T$ is taken as the presolar age of the galaxy, $T^*$ ($= T_G - T_{SS} = 8.7$ Gy), then the ratio $N_{SLR}/N_{Stable}$ in the interstellar medium (ISM) at the time of isolation of the protosolar molecular cloud from fresh nucleosynthetic input can be calculated. This value can be compared to the $N_{SLR}/N_{Stable}$ ratio in the ESS as obtained from meteoritic measurements. The difference between the two values is often interpreted as a "free-decay interval" ($\Delta$) between the last nucleosynthetic event that produced the SLR and the formation of the SS

$$\left(\frac{N_{SLR}}{N_{Stable}}\right)_{ESS} = \left(\frac{N_{SLR}}{N_{Stable}}\right)_{ISM} \cdot e^{\left(-\frac{\Delta}{\tau}\right)} \qquad (2)$$

At present, the meteoritic abundances of only three short-lived *r*-nuclides ($^{129}I$, $^{182}Hf$, and $^{244}Pu$) have been estimated, yielding three different $\Delta$ values (100 ± 7 My, ~35 My, and 158 ± 85 My, respectively) (*7*). The limit of our understanding of the *r*-process is illustrated by the fact that there have been as many *r*-processes proposed as short-lived *r*-nuclides investigated.

Using the value of $(^{247}Cm/^{232}Th)_{ESS} = (1.6 \pm 0.4) \times 10^{-5}$ obtained in this study and the open nonlinear GCE model of Dauphas *et al.* (*28*) with $k = 1.7$, we obtained a free-decay interval of $\Delta = 87 \pm 14$ My. This value is in agreement with the $\Delta$ value of ~100 My derived from $^{129}I$ and $^{244}Pu$ but is much longer than the value of ~35 My obtained from $^{107}Pd$ and $^{182}Hf$ (Fig. 3). If $^{107}Pd$ and $^{182}Hf$ are indeed pure *r*-process isotopes, then a multiplicity of *r*-process environments is needed to explain the inconsistent $\Delta$ values (*5*, *7*). This is evident when looking at Fig. 3: $^{107}Pd$ and $^{129}I$ have similar $(N_{SLR}/N_{Stable})/(P_{SLR}/P_{Stable})$ ratios but

different half-lives, making it impossible for both isotopes to be produced in a single event/process, no matter what model is used for the evolution of the SLR abundances in the giant molecular cloud parental to the SS [for example, free-decay interval versus three-phase mixing ISM (*8*, *30*)]. However, recent nucleosynthetic models have reconsidered the origin of $^{107}$Pd and $^{182}$Hf and find a significant *s*-process contribution (70 to 80%) for both isotopes (*6*, *31*). In such a framework, the initial abundance of all *r*-process SLR in the ESS can be explained by a single *r*-process environment, which last injected material into the protosolar molecular cloud ~100 My before SS formation.

Although some low metallicity halo stars point to the existence of at least three distinct *r*-processes, these stars formed from a gas that had been enriched in *r*-process nuclides by synthesis in very low metallicity stars formed early in the history of the galaxy. Meteorite evidence suggests that such *r*-process multiplicity may only be relevant to exotic conditions that prevailed in the earliest generation of stars in the history of the galaxy and that a single *r*-process may still be relevant to long-term models of the chemical evolution of the galaxy.

## MATERIALS AND METHODS

Twelve fine-grained and three coarse-grained CAIs were selected for this study (fig. S1). One of the coarse-grained CAIs (TS32) was obtained in powder form directly and was described in a previous publication (*32*). All other CAIs were identified in Allende slabs and extracted with clean stainless steel dental tools before digestion by acids. A small chip of each CAI (all but TS32) was extracted using clean stainless steel dental tools under a stereoscopic zoom microscope, and mounted in epoxy for characterization.

All samples were mapped using a JEOL JSM-5800LV scanning electron microscope (SEM). Images of a selected field of view of each CAI, secondary electron, backscattered electron, and false-color RGB (Mg/Ca/Al) are shown in figs. S2 to S15. The REE patterns of the samples were determined using a Quadrupole LA-ICPMS (laser ablation inductively coupled plasma mass spectrometry) at the Field Museum. Diagnostic group II REE patterns were identified in all 12 fine-grained CAIs, indicating that the Nd/U ratio (a proxy for the Cm/U ratio) of these samples was high and that these samples were therefore well suited to search for $^{235}$U excesses coming from $^{247}$Cm decay.

After digestion but before column chemistry, a small aliquot of each sample (~2 to 3%) was used to determine U and REE concentrations. The samples were spiked with IRMM-3636 U double spike ($^{233}$U-$^{236}$U) and processed through U/TEVA resin (Eichrom) column chromatography, using Optima-grade and sub-boiling double-distilled acids.

Isotopic analyses were performed on a ThermoFinnigan Neptune MC-ICPMS at the Origins Lab (University of Chicago), equipped with an OnToolBooster 150 Jet Pump (Pfeiffer) and using Jet sample cones and X skimmer cones. An Aridus II desolvating nebulizer was used for sample introduction, and the measurements were done using a static cup configuration [see (*21*)]. When a ~+55‰ $^{235}$U excess was discovered in the Curious Marie CAI, a new measurement setup was developed that allowed characterization of the U isotopic composition of 0.1 to 0.01 ng of U with a precision of ±2 to 3‰ (see the Supplementary Materials). Extensive testing was done to ensure that no systematic bias was affecting the data, the details of which can be found in the Supplementary Materials.

## SUPPLEMENTARY MATERIALS

Supplementary material for this article is available at http://advances.sciencemag.org/cgi/content/full/2/3/e1501400/DC1

Materials and Methods

Curious Marie: not a FUN CAI.

The $^{247}$Cm-$^{235}$U chronometer and the initial abundances of $^{247}$Cm in the ESS.

GCE model

Fig. S1. Photos of typical fine-grained and coarse-grained CAIs.

Figs. S2 to S15. Secondary electron, backscattered electron, and false-color RGB maps of all samples.

Fig. S16. REE and U-Th abundance patterns of all 12 fine-grained CAIs analyzed in this study.

Fig. S17. Results of the standard addition measurements conducted on the Curious Marie CAI.

Fig. S18. U blank from new U/TEVA resin as a function of the volume of 0.05 M HCl passed through the column.

Fig. S19. Results of precision tests of U isotopic measurements done using various instrumental setups.

Fig. S20. Comparison of the $\delta^{235}$U determined on the CAIs using 80% (*x* axis) and 20% (*y* axis) of the sample.

Fig. S21. Flowchart of the tests conducted on the Curious Marie CAI.

Fig. S22. Evolution of the U isotopic composition of the gas, instantaneous solid, and cumulative solid, as a function of the fraction of U condensed.

Table S1. Results of SEM analysis on small chips of CAIs mounted in epoxy (wt %).

Table S2. Summary of U isotopic compositions and concentrations of CAIs and geostandards.

Table S3. Specifics of U isotopic measurements on MC-ICPMS for low U samples.

Table S4. Compilation of chemistry blanks and effect on U "stable" isotope ratio measurements.

Table S5. Summary of the Ti data obtained on geostandards and the Curious Marie CAI.

Table S6. Production ratios of selected SLRs produced by the *s*-, *r*-, and *p*-process and present in the ESS, normalized to a stable isotope produced in the same or similar nucleosynthetic process.

Table S7. Compilation of Cm/U isochron data and free-decay interval data from experimental and theoretical studies.

Table S8. Selected extinct radionuclides produced by the *s*-, *r*-, and *p*-process.

References (*38*–*78*)

## REFERENCES AND NOTES


1. E. M. Burbidge, G. R. Burbidge, W. A. Fowler, F. Hoyle, Synthesis of the elements in stars. *Rev. Mod. Phys.* **29**, 547–650 (1957).
2. A. G. W. Cameron, *Stellar Evolution, Nuclear Astrophysics, and Nucleogenesis* (Dover Publications Inc., New York, ed. 2, 1957).
3. S. Bisterzo, C. Travaglio, R. Gallino, M. Wiescher, F. Käppeler, Galactic chemical evolution and solar *s*-process abundances: Dependence on the $^{13}$C-pocket structure. *Astrophys. J* **787**, (2014).
4. T. Rauscher, N. Dauphas, I. Dillmann, C. Fröhlich, Z. Fülöp, G. Gyürky, Constraining the astrophysical origin of the p-nuclei through nuclear physics and meteoritic data. *Rep. Prog. Phys.* **76**, 066201 (2013).
5. G. J. Wasserburg, M. Busso, R. Gallino, Abundances of actinides and short-lived nonactinides in the interstellar medium: Diverse supernova sources for the *r*-processes. *Astrophys. J* **466**, L109–L113 (1996).
6. B. S. Meyer, D. D. Clayton, Short-lived radioactivities and the birth of the Sun. *Space Sci. Rev.* **92**, 133–152 (2000).
7. N. Dauphas, Multiple sources or late injection of short-lived *r*-nuclides in the early solar system? *Nucl. Phys. A* **758**, 757–760 (2005).
8. G. R. Huss, B. S. Meyer, G. Srinivasan, J. N. Goswami, S. Sahijpal, Stellar sources of the short-lived radionuclides in the early solar system. *Geochim. Cosmochim. Acta.* **73**, 4922–4945 (2009).
9. V. Hill, B. Plez, R. Cayrel, T. C. Beers, B. Nordström, J. Andersen, M. Spite, F. Spite, B. Barbuy, P. Bonifacio, E. Depagne, P. François, F. Primas, First stars. I. The extreme *r*-element rich, iron-poor halo giant CS 31082-001: Implications for the *r*-process site(s) and radioactive cosmochronology. *Astron. Astrophys.* **387**, 560–579 (2002).
10. L. R. Nittler, N. Dauphas, *Meteorites and the Chemical Evolution of the Milky Way* (University of Arizona Press, Tucson, AZ, 2006), vol. 943, pp. 127–146.
11. G. A. Brennecka, S. Weyer, M. Wadhwa, P. E. Janney, J. Zipfel, A. D. Anbar, $^{238}$U/$^{235}$U variations in meteorites: Extant $^{247}$Cm and implications for Pb-Pb dating. *Science* **327**, 449–451 (2010).
12. G. W. Lugmair, K. Marti, Sm–Nd–Pu time-pieces in Angra dos Reis meteorite. *Earth Planet Sc. Lett.* **35**, 273–284 (1977).
13. W. V. Boynton, Fractionation in solar nebula, II. Condensation of Th,U, Pu and Cm. *Earth Planet Sc. Lett.* **40**, 63–70 (1978).

14. J. H. Jones, The geochemical coherence of Pu and Nd and the $_{244}Pu/_{238}U$ ratio of the early solar system. *Geochim. Cosmochim. Acta.* **46**, 1793–1804 (1982).
15. J. H. Jones, D. S. Burnett, Experimental geochemistry of Pu and Sm and the thermodynamics of trace element partitioning. *Geochim. Cosmochim. Acta.* **51**, 769–782 (1987).
16. M. Tatsumoto, T. Shimamura, Evidence for live $^{247}$Cm in the early Solar System. *Nature* **286**, 118–122 (1980).
17. Y. Amelin, A. Kaltenbach, T. Iizuka, C. H. Stirling, T. R. Ireland, M. Petaev, S. B. Jacobsen, U–Pb chronology of the Solar System's oldest solids with variable $^{238}U/^{235}U$. *Earth Planet Sc. Lett.* **300**, 343–350 (2010).
18. J. N. Connelly, M. Bizzarro, A. N. Krot, Å. Nordlund, D. Wielandt, M. A. Ivanova, The absolute chronology and thermal processing of solids in the solar protoplanetary disk. *Science* **338**, 651–655 (2012).
19. A. Goldmann, G. Brennecka, J. Noordmann, S. Weyer, M. Wadhwa, The uranium isotopic composition of the Earth and the Solar System. *Geochim. Cosmochim. Acta.* **148**, 145–158 (2015).
20. M. B. Andersen, T. Elliott, H. Freymuth, K. W. W. Sims, Y. Niu, K. A. Kelley, The terrestrial uranium isotope cycle. *Nature* **517**, 356–359 (2015).
21. F. L. H. Tissot, N. Dauphas, Uranium isotopic compositions of the crust and ocean: Age corrections, U budget and global extent of modern anoxia. *Geochim. Cosmochim. Acta.* **167**, 113–143 (2015).
22. W. V. Boynton, Fractionation in solar nebula; Condensation of yttrium and rare-earth elements. *Geochim. Cosmochim. Acta.* **39**, 569–584 (1975).
23. A. M. Davis, L. Grossman, Condensation and fractionation of rare earths in the solar nebula. *Geochim. Cosmochim. Acta.* **43**, 1611–1632 (1979).
24. D. K. Ross, J. I. Simon, S. B. Simon, L. Grossman, *The 46th Lunar and Planetary Science Conference*, The Woodlands, Texas, 16 to 20 March 2015.
25. S. S. Russell, G. J. MacPherson, in *Workshop on parent-body and nebular modification of chondritic materials*, Hawaii, 1997, pp. 4054.
26. J. H. Chen, G. J. Wasserburg, The isotopic composition of uranium and lead in Allende inclusions and meteoritic phosphates. *Earth Planet Sc. Lett.* **52**, 1–15 (1981).
27. D. D. Clayton, Galactic chemical evolution and nucleocosmochronology—Standard model with terminated infall. *Astrophys. J* **285**, 411–425 (1984).
28. N. Dauphas, T. Rauscher, B. Marty, L. Reisberg, Short-lived *p*-nuclides in the early solar system and implications on the nucleosynthetic role of X-ray binaries. *Nucl. Phys. A* **719**, C287–C295 (2003).
29. D. D. Clayton, Nuclear cosmochronology within analytic models of the chemical evolution of the solar neighbourhood. *Mon. Not. R. Astron. Soc.* **234**, 1–36 (1988).
30. D. D. Clayton, Extinct radioactivities; A three-phase mixing model. *Astrophys. J* **268**, 381–384 (1983).
31. M. Lugaro, A. Heger, D. Osrin, S. Goriely, K. Zuber, A. I. Karakas, B. K. Gibson, C. L. Doherty, J. C. Lattanzio, U. Ott, Stellar origin of the $^{182}$Hf cosmochronometer and the presolar history of solar system matter. *Science* **345**, 650–653 (2014).
32. S. B. Simon, A. M. Davis, L. Grossman, Origin of compact type A refractory inclusions from CV3 carbonaceous chondrites. *Geochim. Cosmochim. Acta.* **63**, 1233–1248 (1999).
33. C. H. Stirling, A. N. Halliday, D. Porcell, In search of live $^{247}$Cm in the early solar system. *Geochim. Cosmochim. Acta.* **69**, 1059–1071 (2005).
34. C. H. Stirling, A. N. Halliday, E.-K. Potter, M. B. Andersen, B. Zanda, A low initial abundance of $^{247}$Cm in the early solar system and implications for *r*-process nucleosynthesis. *Earth Planet Sc. Lett.* **251**, 386–397 (2006).
35. L. Grossman, R. Ganapathy, Trace elements in Allende meteorite—I. Coarse-grained, Ca-rich inclusions. *Geochim. Cosmochim. Acta.* **40**, 331–344 (1976).
36. L. Grossman, R. Ganapathy, A. M. Davis, Trace elements in the Allende meteorite—III. Coarse-grained inclusions revisited. *Geochim. Cosmochim. Acta* **41**, 1647–1664 (1977).
37. B. Mason, S. R. Taylor, Inclusions in the Allende meteorite, in *Smithsonian Contributions to the Earth Sciences* (Smithsonian Institution Press, Washington, DC, 1982), vol. 25.
38. L. Grossman, Petrography and mineral chemistry of Ca-rich inclusions in Allende meteorite. *Geochim. Cosmochim. Acta.* **39**, 433–434 (1975).
39. G. J. MacPherson, S. B. Simon, A. M. Davis, L. Grossman, A. N. Krot, in *Chondrites and the Protoplanetary Disk,* A. N. Krot, E. R. D. Scott, B. Reipurth, Eds. (University of Michigan, Ann Arbor, MI, 2005), vol. 341, pp. 225.
40. T. Tanaka, A. Masuda, Rare-earth elements in matrix, inclusions, and chondrules of Allende meteorite. *Icarus* **19**, 523–530 (1973).
41. L. Grossman, R. Ganapathy, Trace elements in Allende meteorite—II. Fine-grained. Ca-rich inclusions. *Geochim. Cosmochim. Acta* **40**, 967–977 (1976).
42. K. P. Jochum, U. Weis, B. Stoll, D. Kuzmin, Q. Yang, I. Raczek, D. E. Jacob, A. Stracke, K. Birbaum, D. A. Frick, D. Günther, J. Enzweiler, Determination of reference values for NIST SRM 610–617 glasses following ISO guidelines. *Geostand. Geoanal. Res.* **35**, 397–429 (2011).
43. A. Verbruggen *et al.*, "Preparation and certification of IRMM-3636, IRMM-3636a and IRMM-3636b," JRC Scientific and Technical Reports, 2008.
44. S. Weyer, A. D. Anbar, A. Gerdes, G. W. Gordon, T. J. Algeo, E. A. Boyle, Natural fractionation of $^{238}U/^{235}U$. *Geochim. Cosmochim. Acta.* **72**, 345–359 (2008).
45. T. Meisel, J. Moser, N. Fellner, W. Wegscheider, R. Schoenberg, Simplified method for the determination of Ru, Pd, Re, Os, Ir and Pt in chromitites and other geological materials by isotope dilution ICP-MS and acid digestion. *Analyst* **126**, 322–328 (2001).
46. M. Telus, N. Dauphas, F. Moynier, F. L. H. Tissot, F.-Z. Teng, P. I. Nabelek, P. R. Craddock, L. A. Groat, Iron, zinc, magnesium and uranium isotopic fractionation during continental crust differentiation: The tale from migmatites, granitoids, and pegmatites. *Geochim. Cosmochim. Acta.* **97**, 247–265 (2012).
47. N. Dauphas, A. Pourmand, F.-Z. Teng, Routine isotopic analysis of iron by HR-MC-ICPMS: How precise and how accurate? *Chem. Geol.* **267**, 175–184 (2009).
48. H. Tang, N. Dauphas, Abundance, distribution, and origin of $^{60}$Fe in the solar protoplanetary disk. *Earth Planet Sc. Lett.* **359–360**, 248–263 (2012).
49. T. Lee, T. K. Mayeda, R. N. Clayton, Oxygen isotopic anomalies in Allende Inclusion Hal. *Geophys. Res. Lett.* **7**, 493–496 (1980).
50. H. Nagasawa, D. P. Blanchard, H. Shimizu, A. Masuda, Trace element concentrations in the isotopically unique Allende inclusion, EK 1-4-1. *Geochim. Cosmochim. Acta.* **46**, 1669–1673 (1982).
51. B. Dominik, E.-K. Jessberger, T. Staudacher, K. Nagel, A. El Goresy, in *Lunar and Planetary Institute Science Conference Abstracts* (Lunar and Planetary Institute, Houston, 1978), vol. 9, pp. 1249–1266.
52. A. N. Krot, K. Nagashima, G. J. Wasserburg, G. R. Huss, D. Papanastassiou, A. M. Davis, I. D. Hutcheon, M. Bizzarro, Calcium-aluminum-rich inclusions with fractionation and unknown nuclear effects (FUN CAIs): I. Mineralogy, petrology, and oxygen isotopic compositions. *Geochim. Cosmochim. Acta.* **145**, 206–247 (2014).
53. H. Tang, M. C. Liu, K. D. McKeegan, F. L. H. Tissot, N. Dauphas, Oxygen isotopes and high mg-26 excesses in a u-depleted fine-grained allende cai. *Meteorit. Planet. Sci.* **50**, (2015).
54. R. N. Clayton, R. W. Hinton, A. M. Davis, Isotopic variations in the rock-forming elements in meteorites. *Philos. T. R. Soc. A* **325**, 483–501 (1988).
55. J. B. Blake, D. N. Schramm, 247Cm as a short-lived r-process chronometer. *Nature* **243**, 138–140 (1973).
56. B. Bourdon, S. Turner, G. M. Henderson, C. C. Lundstrom, Introduction to U-series geochemistry. *Rev. Mineral. Geochem.* **52**, 1–21 (2003).
57. G. J. MacPherson, A. M. Davis, Refractory inclusions in the prototypical CM chondrite, Mighei. *Geochim. Cosmochim. Acta.* **58**, 5599–5625 (1994).
58. N. Dauphas, J. H. Chen, J. Zhang, D. A. Papanastassiou, A. M. Davis, C. Travaglio, Calcium-48 isotopic anomalies in bulk chondrites and achondrites: Evidence for a uniform isotopic reservoir in the inner protoplanetary disk. *Earth Planet Sc. Lett.* **407**, 96–108 (2014).
59. F. M. Richter, A. M. Davis, D. S. Ebel, A. Hashimoto, Elemental and isotopic fractionation of Type B calcium-, aluminum-rich inclusions: Experiments, theoretical considerations, and constraints on their thermal evolution. *Geochim. Cosmochim. Acta.* **66**, 521–540 (2002).
60. F. M. Richter, Timescales determining the degree of kinetic isotope fractionation by evaporation and condensation. *Geochim. Cosmochim. Acta.* **68**, 4971–4992 (2004).
61. C. Arlandini, F. Käppeler, K. Wisshak, R. Gallino, M. Lugaro, M. Busso, O. Straniero, Neutron capture in low-mass asymptotic giant branch stars: Cross sections and abundance signatures. *Astrophys. J.* **525**, 886–900 (1999).
62. N. Dauphas, The U/Th production ratio and the age of the Milky Way from meteorites and Galactic halo stars. *Nature* **435**, 1203–1205 (2005).
63. S. Goriely, M. Arnould, Actinides: How well do we know their stellar production? *Astron. Astrophys.* **379**, 1113–1122 (2001).
64. S. B. Jacobsen, *Chondrites and the Protoplanetary Disk*, A. N. Krot, E. R. D. Scott, B. Reipurth, Eds. (ASP, San Francisco, 2005), vol. 341, pp. 548.
65. E. Anders, N. Grevesse, Abundances of the elements: Meteoritic and solar. *Geochim. Cosmochim. Acta.* **53**, 197–214 (1989).
66. M. Boyet, R. W. Carlson, M. Horan, Old Sm–Nd ages for cumulate eucrites and redetermination of the solar system initial $^{146}Sm/^{144}Sm$ ratio. *Earth Planet Sc. Lett.* **291**, 172–181 (2010).
67. R. H. Brazzle, O. V. Pravdivtseva, A. P. Meshik, C. M. Hohenberg, Verification and interpretation of the I-Xe chronometer. *Geochim. Cosmochim. Acta.* **63**, 739–760 (1999).
68. C. Burkhardt, T. Kleine, B. Bourdon, H. Palme, J. Zipfel, J. M. Friedrich, D. S. Ebel, Hf–W mineral isochron for Ca,Al-rich inclusions: Age of the solar system and the timing of core formation in planetesimals. *Geochim. Cosmochim. Acta.* **72**, 6177–6197 (2008).
69. J. H. Chen, G. J. Wasserburg, in *Earth Processes: Reading the Isotopic Code*, A. Basu, S. Hart, Eds. (American Geophysical Union, Washington, D.C., 1996), pp. 1–20.
70. C. L. Harper, Evidence for $^{92}$gNb in the early solar system and evaluation of a new p-process cosmochronometer from $^{92g}Nb/^{92}Mo$. *Astrophys. J.* **466**, 437–456 (1996).
71. G. B. Hudson, B. M. Kennedy, F. A. Podosek, C. M. Hohenberg, in *Lunar and Planetary Institute Science Conference Abstracts* (Lunar and Planetary Institute, Houston, TX, 1989), vol. 19, pp. 547–557.
72. T. Kleine, C. Münker, K. Mezger, H. Palme, Rapid accretion and early core formation on asteroids and the terrestrial planets from Hf–W chronometry. *Nature* **418**, 952–955 (2002).

73. G. W. Lugmair, S. J. G. Galer, Age and isotopic relationships among the angrites Lewis Cliff 86010 and Angra dos Reis. *Geochim. Cosmochim. Acta.* **56**, 1673–1694 (1992).
74. A. Prinzhofer, D. A. Papanastassiou, G. J. Wasserburg, Samarium-neodymium evolution of meteorites. *Geochim. Cosmochim. Acta.* **56**, 797–815 (1992).
75. J. H. Reynolds, Determination of the age of the elements. *Phys. Rev. Lett.* **4**, 8–10 (1960).
76. M. Schönbächler, M. Rehkämper, A. N. Halliday, D.-C. Lee, M. Bourot-Denise, B. Zanda, B. Hattendorf, D. Günther, Niobium-zirconium chronometry and early solar system development. *Science* **295**, 1705–1708 (2002).
77. M. Schönbächler, R. W. Carlson, M. F. Horan, T. D. Mock, E. H. Hauri, Silver isotope variations in chondrites: Volatile depletion and the initial $^{107}$Pd abundance of the solar system. *Geochim. Cosmochim. Acta.* **72**, 5330–5341 (2008).
78. Q. Yin, S. B. Jacobsen, K. Yamashita, J. Blichert-Toft, P. Télouk, F. Albarède, A short timescale for terrestrial planet formation from Hf–W chronometry of meteorites. *Nature* **418**, 949–952 (2002).

**Acknowledgments:** We thank P. Heck, J. Holstein, and the Robert A. Pritzker Center for Meteoritics and Polar Studies at the Field Museum for providing some of the CAI samples; I. Steele for help in operating the SEM at the University of Chicago; and L. Dussubieux for help in operating the LA-ICPMS at the Field Museum. We are grateful to A. M. Davis and B. S. Meyer for discussions. **Funding:** This work was supported by grants from NASA (Laboratory Analysis of Returned Samples, NNX14AK09G; Cosmochemistry, OJ-30381-0036A and NNX15AJ25G) and NSF (Petrology and Geochemistry, EAR144495; Cooperative Studies of the Earth's Deep Interior, EAR150259) to N.D. and a NASA grant (Cosmochemistry, NNX13AE73G) to L.G. **Author contributions:** N.D. and F.L.H.T. designed the research; F.L.H.T. and L.G. selected the samples; F.L.H.T. performed the research; F.L.H.T., N.D., and L.G. wrote the paper. **Competing interests:** The authors declare that they have no competing interests. **Data and materials availability:** All data needed to evaluate the conclusions in the paper are present in the paper and/or the Supplementary Materials. Additional data are available from the authors upon request. This is Origins Lab contribution number 91.

Submitted 7 October 2015
Accepted 12 January 2016
Published 4 March 2016
10.1126/sciadv.1501400

**Citation:** F. L. H. Tissot, N. Dauphas, L. Grossman, Origin of uranium isotope variations in early solar nebula condensates. *Sci. Adv.* **2**, e1501400 (2016).

ScienceAdvances
AAAS

**Origin of uranium isotope variations in early solar nebula condensates**

François L. H. Tissot, Nicolas Dauphas and Lawrence Grossman

(March 4, 2016)
*Sci Adv* 2016, 2:.
doi: 10.1126/sciadv.1501400